Determination of a $^{199}Hg-^{31}P$ Indirect Spin-Spin Coupling Tensor via Single-Crystal Phosphorus NMR Spectroscopy

Michael D. Lumsden,† Klaus Eichele,† Roderick E. Wasylishen,*,† T. Stanley Cameron,† and James F. Britten‡

Contribution from the Department of Chemistry, Dalhousie University, Halifax, Nova Scotia, Canada B3H 4J3, and the Department of Chemistry, McMaster University, Hamilton, Ontario, Canada L8S 4M1

Received May 25, 1994®

Abstract: Both the phosphorus chemical shift (CS) tensor and the $^{199}Hg-^{31}P$ spin-spin coupling tensor have been determined for the 1:1 mercury(II) phosphine complex $HgPCy_3(NO_3)_2$ (Cy = cyclohexyl) (**1**) using single-crystal ^{31}P NMR spectroscopy. The phosphorus CS is found to be anisotropic with a span of approximately 90 ppm. The orientation of the principal axis system of the phosphorus CS tensor has been assigned in the molecular reference frame and is found to conform with the local site symmetry at the phosphorus atom. These results represent the first determination of the complete phosphorus CS tensor in a metal-phosphine complex. The orientation dependence of the $^{199}Hg-^{31}P$ spin-spin coupling has been monitored as a function of crystal orientation in the external magnetic field from which the traceless part of the $^{199}Hg-^{31}P$ **J** tensor has been determined. A significant anisotropy, on the order of 5400 Hz, is found to exist, indicating the participation of non-Fermi contact mechanisms in the electron mediated transmission of nuclear spin information between ^{199}Hg and ^{31}P in **1**. An X-ray crystallographic structure determination has also been performed for **1**, revealing the presence of a polymeric chain structure in contrast to the dimeric species found previously. Crystals of **1** were found to belong to the monoclinic space group $P2_1/c$ with $Z = 4$ and unit cell dimensions $a = 10.360(2)$ Å, $b = 10.247(1)$ Å, $c = 21.005(4)$ Å, $\beta = 97.73(2)°$. The structure was refined using least-squares techniques to a final R-factor of 0.0365 based on 3070 independent reflections.

Introduction

Two nuclei possessing an inherent spin angular momentum can be spin-spin coupled to one another *via* two fundamentally different interactions which are the well-known direct dipolar and indirect spin-spin coupling (J) interactions. Although the dependence of the dipolar interaction on the orientation of a molecule with respect to the external magnetic field is well-established, what has remained more obscure is the fact that J coupling is an orientation-dependent interaction as well.[1-3] In order to fully describe such an orientation-dependent or anisotropic spin-spin coupling, the **J** interaction must be characterized by a second-rank tensor.

Although the literature abounds with investigations involving the application of *isotropic J* couplings to the study of molecular structure, few **J** *tensors* have been characterized. It must be emphasized that a thorough understanding of indirect spin-spin coupling will only be realized once theoretical treatments are able to reproduce and lend insight into reliable experimental determinations of the complete **J** tensor rather than simply its trace. From a theoretical standpoint, such an achievement is indeed non-trivial due qualitatively in part to the extremely small interaction energies involved as well as the dependence of the **J** interaction upon the molecular wave functions for the singlet and triplet excited states within the system under investigation.[1-3] Consequently, a substantial portion of the literature pertaining to the theoretical calculation of J couplings[4] involves semi-empirical implementations of Ramsey's theory, predominantly for nuclei of the first-row main group elements. Unfortunately, like the theoretician, the experimentalist is also confronted with an inherent obstacle in measuring accurate **J** tensors which in part accounts for the profound lack of reliable experimental data in this area. Unlike the situation in traditional solution NMR studies where the isotropic component of the **J** interaction can be measured independently from the traceless dipolar interaction, in ordered systems both the direct dipolar interaction and the anisotropic component of the **J** interaction are manifested in NMR spectra as orientation-dependent splittings.[5-9] For two coupled spins, A and X, the interaction energy is

$$E_{AX} = hJ_{iso}\mathbf{I}_A\cdot\mathbf{I}_X + h\mathbf{I}_A\cdot\mathbf{R}^{eff}\cdot\mathbf{I}_X \quad (1)$$

where J_{iso} is the isotropic indirect spin-spin coupling constant, $\mathbf{R}^{eff}$ is the effective dipolar coupling tensor, and **I** is the total nuclear spin angular momentum vector. The second-rank tensor, $\mathbf{R}^{eff}$, may be expressed as the sum of the direct dipolar coupling

* Address Correspondence to this author.
† Dalhousie University.
‡ McMaster University.
® Abstract published in *Advance ACS Abstracts,* October 15, 1994.

(1) Ramsey, N. F. *Phys. Rev.* **1953**, *91*, 303-307.
(2) Jameson, C. J. In *Phosphorus-31 NMR Spectroscopy in Stereochemical Analysis, Organic Compounds and Metal Complexes*; Verkade, J. G., Quin, L. D., Eds.; Methods in Stereochemical Analysis 8; VCH Publishers, Inc.: Deerfield Beach, FL, 1987; pp 205-230.
(3) Jameson, C. J. In *Multinuclear NMR*; Mason, J., Ed.; Plenum Press: New York, 1987; pp 89-131.
(4) (a) Kowalewski, J. *Progr. Nucl. Magn. Reson. Spectrosc.* **1977**, *11*, 1-78. (b) Kowalewski, J. *Annu. Rep. NMR Spectrosc.* **1982**, *12*, 81-176. (c) Contreras, R. H.; Facelli, J. C. *Annu. Rep. NMR Spectrosc.* **1993**, *27*, 255-356.
(5) (a) VanderHart, D. L.; Gutowsky, H. S. *J. Chem. Phys.* **1968**, *49*, 261-271. (b) VanderHart, D. L.; Gutowsky, H. S.; Farrar, T. C. *J. Chem. Phys.* **1969**, *50*, 1058-1065.
(6) Zilm, K. W.; Grant, D. M. *J. Am. Chem. Soc.* **1981**, *103*, 2913-2922.
(7) Power, W. P.; Wasylishen, R. E. *Annu. Rep. NMR Spectrosc.* **1991**, *23*, 1-84.
(8) Robert, J. B.; Wiesenfeld, L. In *Phosphorus-31 NMR Spectroscopy in Stereochemical Analysis, Organic Compounds and Metal Complexes*; Verkade, J. G., Quin, L. D., Eds.; Methods in Stereochemical Analysis 8; VCH Publishers, Inc.: Deerfield Beach, FL, 1987; pp 151-183.
(9) Wasylishen, R. E. In *Encyclopedia of Nuclear Magnetic Resonance*; Grant, D. M., Harris, R. K., Eds.; John Wiley & Sons, to be published.

0002-7863/94/1516-11129$04.50/0 © 1994 American Chemical Society

tensor, **D**, and the traceless part of the **J** tensor, $\mathbf{J} - J_{iso}\cdot\mathbf{1}$. The direct dipolar tensor can be readily calculated since it depends upon the magnetic moments of the coupled nuclear spins as well as the inverse cube of the *AX* internuclear separation. Conversely, $\mathbf{J} - J_{iso}\cdot\mathbf{1}$ does not depend upon the molecular geometry in any obvious way. It is clear that a reliable determination of a **J** tensor is contingent upon prior knowledge of the corresponding dipolar tensor as well as the relative orientations of these two spin−spin interactions. This, in turn, necessitates knowing accurate values for the internuclear separation between the coupled nuclei within the medium in which the NMR experiment is performed.

Despite these difficulties, it is imperative that experimentalists strive for accurate measurements of **J** tensors given the current status of our understanding of the structural factors that dictate the orientation-dependent nature of *J* couplings. Although the sensitive link between isotropic *J* couplings and molecular structure has long been established and well-exploited, there potentially lies an abundance of untapped molecular and electronic structural information in the three-dimensional nature of *J* couplings. Furthermore; accurate measurements of **J** tensors are essential in order to provide stringent tests of theoretical calculations of *J* couplings. Finally, it is important to emphasize that elucidation of an orientation-dependent *J* coupling implies that the electron-mediated transmission of the nuclear spin information involves mechanisms other than the Fermi contact mechanism.[1-3] The common tendency to assume Fermi contact dominance when calculating and/or interpreting *J* couplings is an axiom which has clearly propagated from the lack of data involving **J** tensors and must be justified.

Traditionally, experimental characterization of **J** tensors has predominantly involved either NMR studies of solute molecules oriented in liquid crystalline solvents[10,11] or analysis of solid-state NMR spectra of slow magic-angle-spinning (MAS)[12] or, preferably, static powder samples.[5,6,13-24] However, each of these approaches is potentially problematic with a successful analysis often contingent upon various assumptions which invariably heighten the experimental uncertainty in the derived **J** tensor. A superior approach for the experimental characterization of indirect spin−spin coupling tensors is the single-crystal NMR technique. The key to the success of this powerful method lies in the fact that for multiple-interaction spin systems, analysis of the coupling data is completely independent of the chemical shift interaction, unlike the situation for powder samples. It is surprising that, to date, there have been only three such single-crystal studies, one of these involving a system where X-ray crystallographic data were unavailable.[25,26] The present study is the fourth such investigation and entails the first complete characterization of a metal−phosphorus indirect spin−spin coupling tensor, namely the one-bond $^{199}Hg-^{31}P$ **J** tensor in the complex $HgPCy_3(NO_3)_2$ (**1**). As well, an X-ray crystallographic structure determination has been performed for this species, enabling reliable calculation of the $^{199}Hg-^{31}P$ direct dipolar coupling tensor.

Experimental Section

Compound Preparation. Bis(nitrato)(tricyclohexylphosphine)-mercury(II), **1**, was prepared by a standard synthetic procedure as described elsewhere.[27] The purity was verified by a melting point determination as well as solution ^{31}P NMR studies. The single crystal used in the NMR studies was obtained by slow evaporation of a dichloromethane solution. The remaining crystals were subsequently ground and used for the acquisition of the spectra obtained for powdered samples of **1**.

X-ray Crystallography. A crystal of approximate dimensions 0.20 × 0.30 × 0.35 mm was cut from the large single crystal used in the NMR study and mounted in a glass capillary. All diffraction measurements were carried out at room temperature on a Rigaku AFC5R diffractometer (Mo Kα, $\lambda = 0.71069$ Å, graphite monochromator) using the $\omega/2\theta$ scan technique, to a maximum 2θ value of 46.0°. A scan speed of 8.0°/min (with 5 rescans) and a scan width of (0.84 + 0.35 tan θ)° were employed. Cell constants and an orientation matrix for data collection obtained from a least-squares refinement using the setting angles of 20 carefully centered reflections in the range $39.63° < 2\theta < 44.38°$ corresponded to a monoclinic cell with dimensions $a = 10.360(2)$ Å, $b = 10.247(1)$ Å, $c = 21.005(4)$ Å, and $\beta = 97.73(2)°$ and crystal data $V = 2209.7(6)$ Å^3, $Z = 4$, and $D_{calc} = 1.819$ g/cm^3. The systematic absent reflections uniquely indicated the space group to be $P2_1/c$ (No. 14). Crystal and electronic stability was monitored by measuring the intensities of three representative reflections after every 150 reflections and was found to remain constant. The data were corrected for Lorentz and polarization effects and an empirical absorption correction was applied, using the program DIFABS,[28] which resulted in transmission factors ranging from 0.842 to 1.398.

The structure was solved by using direct methods to locate the heavy atoms with the remaining atoms positioned from a difference Fourier map. The maximum and minimum peaks in the final map corresponded to 1.332 and −1.702 e Å^{-3}, respectively. The non-hydrogen atoms were refined anisotropically. The hydrogen atoms were placed in their geometrically calculated positions with a C−H distance of 0.95 Å; their positions were refined isotropically. The final cycle of full-matrix least-squares refinement on F^2 [29] was based on 3070 observed reflections ($I > 2.00\sigma(I)$) and 254 variable parameters. Convergence was obtained with $R = 0.0365$. All calculations were performed using the SHELXL-93 crystallographic software package of Crystal Structure Determination running under TEXSAN management.[30]

Solid-State NMR Studies. A single crystal of approximate dimensions 3.5 × 3.0 × 1.0 mm was mounted on a hollow, three-sided alumina cube with axes 4 mm in length. An NMR cube reference frame was defined by arbitrarily labeling the cube axes *X*, *Y*, and *Z* in a right-handed fashion (see Figure 1). The orientation matrix describing the location of the unit cell axes with respect to this reference frame

(10) Emsley, J. W.; Lindon, J. C. *NMR Spectroscopy Using Liquid Crystal Solvents*; Pergamon Press: Oxford, 1975.
(11) Lounila, J.; Jokisaari, J. *Progr. Nucl. Magn. Reson. Spectrosc.* **1982**, *15*, 249−290.
(12) Harris, R. K.; Packer, K. J.; Thayer, A. M. *J. Magn. Reson.* **1985**, *62*, 284−297.
(13) Grimmer, A.-R.; Peter, R.; Fechner, E. *Z. Chem.* **1978**, *18*, 109−110.
(14) Balz, R.; Haller, M.; Hertler, W. E.; Lutz, O.; Nolle, A.; Schafitel, R. *J. Magn. Reson.* **1980**, *40*, 9−16.
(15) Grimmer, A.-R.; Müller, D.; Neels, J. *Z. Chem.* **1983**, *23*, 140−142.
(16) Haubenreisser, U.; Sternberg, U.; Grimmer, A.-R. *Mol. Phys.* **1987**, *60*, 151−163.
(17) Zilm, K. W.; Webb, G. G.; Cowley, A. H.; Pakulski, M.; Orendt, A. *J. Am. Chem. Soc.* **1988**, *110*, 2032−2038.
(18) Penner, G. H.; Power, W. P.; Wasylishen, R. E. *Can. J. Chem.* **1988**, *66*, 1821−1823.
(19) Duchamp, J. C.; Pakulski, M.; Cowley, A. H.; Zilm, K. W. *J. Am. Chem. Soc.* **1990**, *112*, 6803−6809.
(20) Power, W. P.; Lumsden, M. D.; Wasylishen, R. E. *Inorg. Chem.* **1991**, *30*, 2997−3002.
(21) Power, W. P.; Lumsden, M. D.; Wasylishen, R. E. *J. Am. Chem. Soc.* **1991**, *113*, 8257−8262.
(22) Power, W. P.; Wasylishen, R. E. *Inorg. Chem.* **1992**, *31*, 2176−2183.
(23) Wu, G.; Wasylishen, R. E. *J. Phys. Chem.* **1993**, *97*, 7863−7869.
(24) Wasylishen, R. E.; Wright, K. C.; Eichele, K.; Cameron, T. S. *Inorg. Chem.* **1994**, *33*, 407−408.
(25) Nolle, A. *Z. Phys. B* **1979**, *34*, 175−182.
(26) (a) Tutunjian, P. N.; Waugh, J. S. *J. Chem. Phys.* **1982**, *76*, 1223−1226. (b) Tutunjian, P. N.; Waugh, J. S. *J. Magn. Reson.* **1982**, *49*, 155−158.
(27) Alyea, E. C.; Dias, S. A.; Goel, R. G.; Ogini, W. O.; Pilon, P.; Meek, D. W. *Inorg. Chem.* **1978**, *17*, 1697−1700.
(28) Walker, N.; Stuart, D. *Acta Crystallogr.* **1983**, *A39*, 158−166.
(29) Function minimized: $\sum\omega(|F_o| - |F_c|)^2$ where $\omega = p/\sigma^2(F_o)$ ($p = 1.3234$).
(30) SHELXL-93: Program for Crystal Structure Determination; Sheldrick, G. M.; Institut für Anorg. Chemie, Göttingen. As modified locally to run under TEXSAN (MSC Corp., The Woodlands, TX 77381).

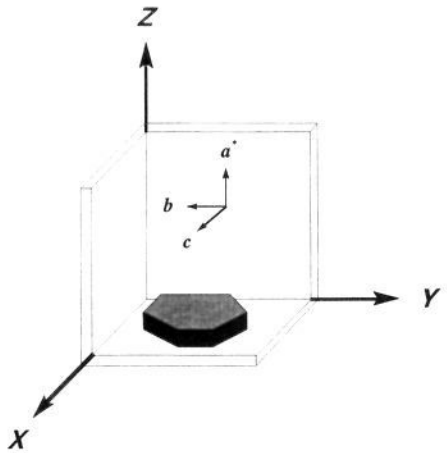

Figure 1. The hollow, three−sided cube in which the single crystal is mounted. The convention used in defining the NMR cube reference frame (X, Y, Z) is illustrated, as well as the relative orientation of the orthogonalized monoclinic crystallographic axis system (a^*, b, c) with respect to the NMR cube reference frame, which is given by the Euler angles $\alpha = 357.5°$, $\beta = 90.6°$, $\gamma = 178.1°$.

was obtained by placing the NMR sample in its alumina cube holder on an X-ray diffractometer and indexing 21 well-centered reflections. The results of this analysis are depicted in Figure 1. Errors in the position of each axis were estimated to be less than 0.5°.

Single-crystal ^{31}P NMR spectra were acquired with a single-crystal goniometer probe from Doty Scientific. Rotation patterns were obtained by rotating the crystal about each of the three orthogonal cube axes within a hollow cubic receptacle in the probe goniometer, with the rotation axis oriented perpendicular to the external field direction. Spectra were obtained for a total of 16 orientations for each rotation pattern, corresponding to rotations from 0° to 90° in 9° increments and from 90° to 180° in 18° increments. The origin of the increased interval size within the latter half of each rotation pattern was due to the excessive time required to obtain the NMR data; the total spectrometer time necessary to complete the single-crystal NMR experimentation was approximately 21 days. This difficulty was, in turn, related to the long proton spin−lattice relaxation times in this sample as well as the need to obtain adequate signal-to-noise ratios in order to define the resonance frequencies of the weak ^{199}Hg satellite peaks. For each orientation, typically 32 free-induction decays were signal averaged with a recycle delay of 20 min and an acquisition time of 10.24 ms. ^{31}P NMR spectra were also obtained for powder samples and were acquired with a Bruker double-air-bearing MAS probe, using 7 mm o.d. zirconium oxide rotors. Experiments involving rotation of the single crystal at the magic angle were also obtained in this fashion.

All ^{31}P NMR spectra were obtained at 81.03 MHz on a Bruker MSL-200 NMR spectrometer employing the FLIPBACK pulse sequence[31] under conditions of cross-polarization and high-power proton decoupling. Proton 90° pulse widths of 3.45 and 3.95 μs were used for the single-crystal and powder spectra, respectively. In all cases, a cross-polarization time of 5 ms was employed. Spectra have been referenced with respect to 85% H_3PO_4 (aq). We maintain the following convention for the principal components of the ^{31}P chemical shift tensors: $\delta_{11} \geq \delta_{22} \geq \delta_{33}$, where δ_{11} and δ_{33} are the least shielded and most shielded components, respectively. The span of the chemical shift tensor, Ω, is defined as $\delta_{11} - \delta_{33}$.[32] The convention used for designating the three principal components of the $^{199}Hg-^{31}P$ **J** coupling tensors is $|J_{zz} - J_{iso}| \geq |J_{xx} - J_{iso}| \geq |J_{yy} - J_{iso}|$.

Calculation of the ^{31}P NMR line shape obtained for a static powder sample of **1** was performed with an 80486 microprocessor and simulation software developed in this laboratory which incorporates the POWDER routine.[33]

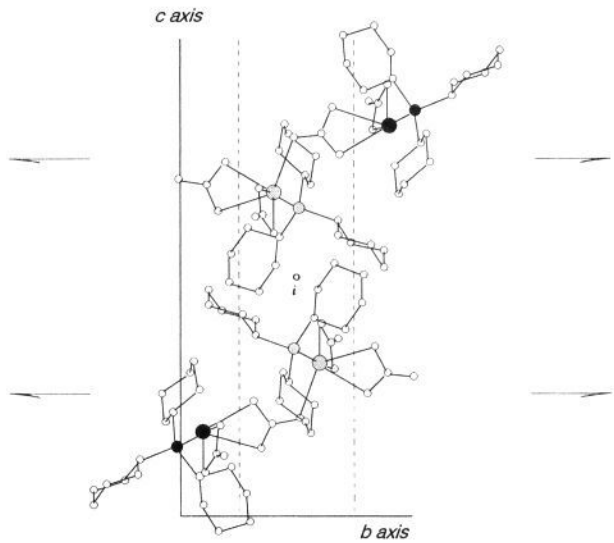

Figure 2. The unit cell of **1**, projected into the crystallographic bc plane. The pertinent space group symmetry elements are also shown. The two magnetically distinct Hg, P spin pairs are indicated by dotted and closed circles for sites 1 and 2, respectively. Hydrogen atoms have been omitted for clarity.

Results and Discussion

Crystal Structure of $HgPCy_3(NO_3)_2$. The structure of **1** is found to consist of $\cdots NO_3 \cdots Hg \cdots NO_3 \cdots$ polymeric chains generated by a 2-fold screw axis parallel to the crystallographic b axis (see Figure 2). The unit cell contains segments of two polymers which are related *via* the c glide plane perpendicular to the b axis. Interestingly, these results can be contrasted with an earlier X-ray analysis involving the species $[HgPCy_3(NO_3)_2]_2$, where it was found that distinct centrosymmetric dimers existed.[34] It appears that the only difference between this earlier study and the present investigation, in terms of crystal isolation, is that the former study used methanol in the recrystallization process. Whether or not this variation is responsible for the apparent structural isomerism is difficult to assess. It should be mentioned that both of these types of structures are common in 1:1 mercury−phosphine complexes.[35] The factors dictating which structure is realized in practice are not entirely understood, although the steric requirements of the associated phosphine ligand are often implicated. For example, it has been suggested that greater phosphine steric hinderance favors the dimeric structure;[34] however, based on the distinct findings for the PCy_3 ligand, such an explanation is certainly not satisfying.

Despite the differences in the bonding modes of the bridging nitrato groups in these species, the coordination geometries at the mercury atoms are often similar and this holds true for **1** as well. However, descriptions of these geometries vary depending on the criterion used to distinguish a "true" Hg−O bond from a mere long-range interaction. In Figure 3, the molecular geometry of **1** is illustrated as well as the atomic numbering scheme used. In Table 1, a series of selected interatomic distances and bond angles are provided. The structure of **1** is analogous to that found previously for the related triphenylphosphine derivative.[35a] Two independent types of nitrato groups are present: a bridging group, containing N(1), involved in the formation of the polymeric chain structure and a second, terminal, bidentate group involving N(2). As in the triphen-

(31) Tegenfeldt, J.; Haeberlen, U. *J. Magn. Reson.* **1979**, *36*, 453−457.
(32) Mason, J. *Solid State Nucl. Magn. Reson.* **1993**, *2*, 285−288.
(33) Alderman, D. W.; Solum, M. S.; Grant, D. M. *J. Chem. Phys.* **1986**, *84*, 3717−3725.
(34) Alyea, E. C.; Dias, S. A.; Ferguson, G.; Restivo, R. J. *Inorg. Chem.* **1977**, *16*, 2329−2334.
(35) See, for example: (a) Whitlow, S. H. *Can. J. Chem.* **1974**, *52*, 198−202. (b) Alyea, E. C.; Dias, S. A.; Ferguson, G.; Parvez, M. *Inorg. Chim. Acta* **1979**, *37*, 45−52.

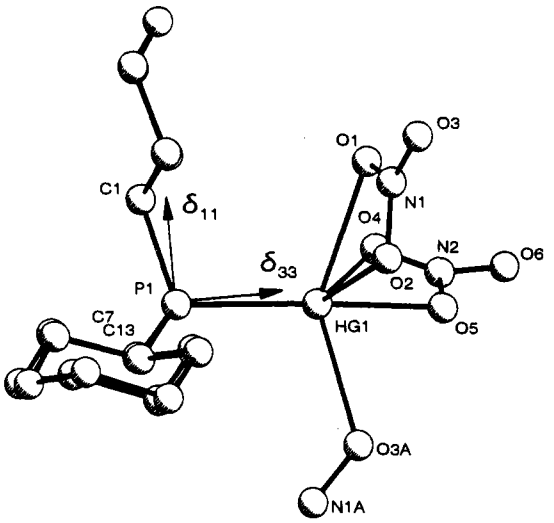

Figure 3. The molecular structure and atomic numbering scheme of the monomeric unit, $HgPCy_3(NO_3)_2$, as determined by X-ray crystallography. Hydrogen atoms have been omitted for clarity. Also displayed is the orientation of the principal axis system of the phosphorus chemical shift tensor in **1** obtained from the single-crystal NMR analysis (*vide infra*). The most shielded principal component, δ_{33}, is oriented 4° off the Hg−P bond axis. The intermediate principal component, δ_{22}, was found to lie perpendicular to the plane of projection.

Table 1. Selected Interatomic Distances and Angles in **1**[a]

	distance (Å)		angle (deg)
Hg(1)−P(1)	2.365(3)	Hg(1)−P(1)−C(1)	108.7(3)
Hg(1)−O(1)	2.591(8)	Hg(1)−P(1)−C(7)	109.4(3)
Hg(1)−O(2)	2.520(8)	Hg(1)−P(1)−C(13)	110.5(4)
Hg(1)−O(3)′	2.579(9)	C(1)−P(1)−C(7)	109.9(5)
Hg(1)−O(4)	2.542(8)	C(1)−P(1)−C(13)	110.8(5)
Hg(1)−O(5)	2.248(7)	C(7)−P(1)−C(13)	107.4(5)
P(1)−C(1)	1.845(11)	P(1)−Hg(1)−O(1)	108.5(2)
P(1)−C(7)	1.848(10)	P(1)−Hg(1)−O(2)	115.9(2)
P(1)−C(13)	1.848(11)	P(1)−Hg(1)−O(3)′	104.5(2)
N(1)−O(1)	1.239(14)	P(1)−Hg(1)−O(4)	114.4(3)
N(1)−O(2)	1.291(13)	P(1)−Hg(1)−O(5)	163.6(3)
N(1)−O(3)	1.243(13)	O(1)−Hg(1)−O(2)	47.4(4)
N(2)−O(4)	1.23(2)	Hg(1)−O(2)−N(1)	102.7(7)
N(2)−O(5)	1.278(14)	O(1)−N(1)−O(2)	108.7(10)
N(2)−O(6)	1.212(14)	O(1)−N(1)−O(3)	128.4(11)
average C−C	1.53	O(2)−N(1)−O(3)	122.9(11)
		O(4)−Hg(1)−O(5)	51.5(4)
		Hg(1)−O(5)−N(2)	103.8(7)
		O(4)−N(2)−O(5)	113.8(10)
		O(4)−N(2)−O(6)	132.3(14)
		O(5)−N(2)−O(6)	113.7(14)
		average C−C−C	110.9

[a] Primed atoms refer to the following transformation: $-x + 1, y - 1/2, -z + 1/2$.

ylphosphine complex, there appears to be an inverse correlation within these groups between the N−O bond lengths and the corresponding Hg−O separations. The terminal nitrato group, as in the triphenylphosphine analogue, is more strongly coordinated to the mercury, which is reflected in a short Hg−O(5) bond (2.25 Å) and long N(2)−O(5) bond (1.28 Å). This stronger coordination is also reflected in the asymmetry in the bond angles within this group (*i.e.* Hg−O(4)−N(2) 91° and Hg−O(5)−N(2) 104°). Interestingly, this asymmetric behavior is not as strong as in the related triphenylphosphine complex, which results in a relatively short Hg−O(4) bond compared with the PPh_3 species (2.54 Å in **1** *vs.* 2.69 Å in the PPh_3 complex). Given the sum of the van der Waals radii of Hg and O (1.5 Å for each),[36] the bidentate nature of this group is apparent. The bridging nitrato group is, however, remarkably more symmetrical, which is manifested in the relatively similar Hg−O distances and N−O bonds as well as Hg−O−N bond angles (*i.e.* Hg−O(1)−N(1) 101° and Hg−O(2)−N(1) 103°). This result is in sharp contrast with the triphenylphosphine analogue, in which the corresponding nitrato group is unidentate with Hg−O distances of 2.56 and 2.94 Å.[35a] Whether this group in **1** is considered uni- or bidentate is debatable. If unidentate, the mercury coordination geometry could be described as distorted square pyramidal with O(2) at the apex, which is more common than hexacoordination. However, considering the sum of the van der Waals radii for Hg and O, this higher coordination number cannot be ruled out.

The anisotropic thermal parameters of oxygen atoms O(1), O(3), O(4), and O(6) of the two nitrato groups are all somewhat larger than those of the other atoms, indicating that they are either slightly disordered or that there is a significant libration about the N(1)−O(2) and N(2)−O(5) axes, respectively. This is a probable cause of the apparent shortening of the N(1)−O(1), N(1)−O(3), N(2)−O(4), and N(2)−O(6) bonds. Unfortunately, the atoms lie on the surface of a conic section and under these circumstances true libration corrections should not and have not been applied to the bond lengths. Regardless of the type of motion occurring within the nitrato groups, this is expected to have no observable effect on the NMR tensors obtained in the present investigation.

The coordination geometry at the phosphorus atom is essentially tetrahedral with Hg−P−C angles ranging from 109° to 111° and C−P−C angles varying from 107° to 111°. The Hg−P bond length, 2.365 Å, is virtually identical with that in the dimeric isomer, as is the average C−C bond length, 1.53 Å, and C−C−C angle, 111°. Each of the cyclohexane rings adopts the chair conformation.

Phosphorus Chemical Shift Tensors. As illustrated in Figure 2, the unit cell of **1** contains four crystallographically equivalent phosphorus nuclei. Each pair of phosphorus nuclei related by either a 2_1 axis or a *c* glide plane is magnetically non-equivalent in the NMR experiment.[37] However, the remaining two possible pairs consist of magnetically equivalent ^{31}P nuclei due to the presence of an inversion center. Consequently, for a general orientation of a single crystal of **1** in an external magnetic field, peaks from two magnetically distinct sites (arbitrarily designated sites 1 and 2 in Figure 2) are observed. This is illustrated in Figure 4, which shows the ^{31}P single-crystal NMR spectrum obtained for the *X*(81°) orientation. For each site, a total of three peaks are obtained: a strong central peak due to ^{31}P nuclei that are adjacent to mercury isotopes with spin $I = 0$ and two much weaker satellite peaks resulting from ^{31}P nuclei that are spin−spin coupled to ^{199}Hg nuclei ($I = 1/2$, natural abundance = 16.84%). Although the mercury isotope ^{201}Hg also possesses a non-zero spin angular momentum ($I = 3/2$, natural abundance = 13.22%), no evidence of ^{201}Hg−^{31}P spin−spin coupling was apparent in the single-crystal ^{31}P NMR spectra obtained in this study. The variation in resonance frequency of the uncoupled ^{31}P peaks or, equivalently, the average frequencies of the ^{199}Hg satellite peaks with orientation of the single crystal in the external magnetic field is solely a function of the anisotropic phosphorus chemical shielding interaction. Consequently, by monitoring the positions of the chemical shifts for rotations about the three orthogonal cube

(36) Huheey, J. E. *Inorganic Chemistry, Principles of Structure and Reactivity*; Harper & Row Publishers, Inc.: New York, 1983; pp 258−259.

(37) Haeberlen, U. In *Advances in Magnetic Resonance, Supplement 1*; Waugh, J. S., Ed.; Academic Press: New York, 1976.

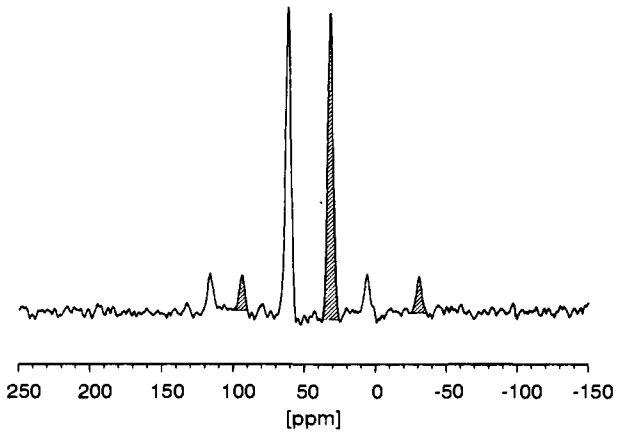

Figure 4. A representative ^{31}P single-crystal NMR spectrum obtained for the $X(81°)$ orientation of the single crystal of **1** in the external magnetic field. Peaks arising from the two magnetically non-equivalent sites (*cf.* Figure 2) have been distinguished by open and dashed lines for sites 1 and 2, respectively.

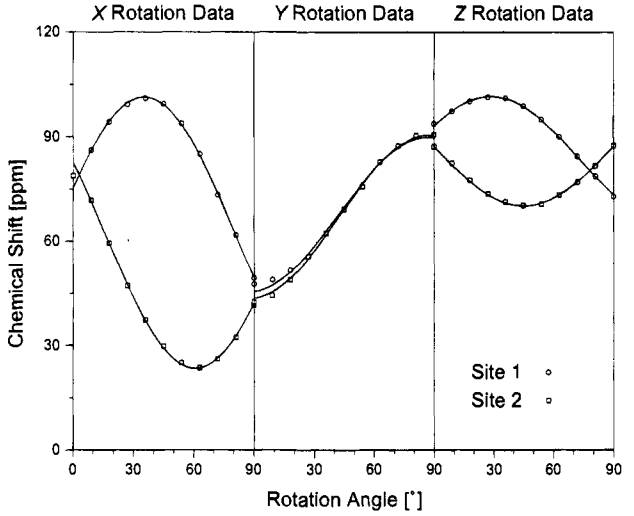

Figure 5. NMR single-crystal rotation plots displaying the variation in the phosphorus chemical shift for rotations about the cube *X*, *Y*, and *Z* axes, as indicated. The data obtained for each magnetically non-equivalent site are labeled according to the scheme depicted in Figure 2.

axes perpendicular to the external field direction, the phosphorus chemical shift (CS) tensor can be constructed,[37−41] which will be the focus of the remainder of this section. Similarly, the anisotropy in the **splittings** of the satellite peaks can be analyzed, independent of the CS interaction, to obtain the sum of the $^{199}Hg-^{31}P$ direct and indirect spin−spin coupling tensors, the discussion of which will be reserved for the following section.

Rotation plots displaying the variation in CS of the two magnetically distinct ^{31}P nuclei for rotation about each of the three orthogonal NMR cube axes are shown in Figure 5. The data have been analyzed in the conventional manner;[42] note that small phase angles, ξ, of magnitude $-2°$ and $+3°$ have been applied to the *X* and *Z* rotation data, respectively.[43] The results of the CS tensor analyses are summarized in Table 2. Note

Table 2. Phosphorus Chemical Shift Tensor Data for $HgPCy_3(NO_3)_2$ Obtained from Analysis of the Single-Crystal NMR Data[a]

		chemical shift (ppm)[b,c]	direction cosines[d]		
site 1	δ_{11}	110	−0.363	−0.704	−0.606
	δ_{22}	83	−0.422	−0.461	0.784
	δ_{33}	20	−0.831	0.541	−0.134
	$^1/_3\Sigma\delta_{ii}$	71			
site 2	δ_{11}	112	−0.397	0.761	−0.518
	δ_{22}	83	−0.412	0.351	0.838
	δ_{33}	23	0.820	0.545	0.170
	$^1/_3\Sigma\delta_{ii}$	72			

[a] The convention used for designating the three principal components of the CS tensor is $\delta_{11} \geq \delta_{22} \geq \delta_{33}$, where δ_{11} and δ_{33} are the least shielded and most shielded principal components, respectively. [b] All chemical shifts are referenced with respect to 85% H_3PO_4 (aq) at 0 ppm. [c] Errors in the principal components of the ^{31}P CS tensors are estimated to be 1 ppm. [d] The direction cosines are with respect to the orthogonalized crystallographic frame (a^*, b, c).

that the average of the three principal components of the CS tensor for each site is in very good agreement with the isotropic chemical shift obtained from a ^{31}P MAS NMR spectrum for a powder sample of **1**, $\delta_{iso} = 72.2$ ppm. It is interesting to note that the isotropic phosphorus CS obtained here is approximately 7 ppm more shielded than that obtained for a 1:1 mercury−tricyclohexylphosphine complex ($\delta_{iso} = 79.5$ ppm) in an earlier ^{31}P NMR investigation,[21] which may represent the isotropic ^{31}P CS in the dimeric structural isomer.

The final step in this analysis involved the transformation of each CS tensor principal axis system into the molecular frame. Although there exists a 2-fold ambiguity in assigning the tensors to an individual site within the unit cell, this was resolved by making use of the corresponding orientations of the $^{199}Hg-^{31}P$ effective coupling tensors (*vide infra*) as well as local symmetry considerations. As for the former argument, one intuitively anticipates that the unique component of the $^{199}Hg-^{31}P$ coupling tensor will be oriented close to the Hg−P bond axis. Examination of both possible assignments of the coupling tensors to the two magnetically distinct sites within the unit cell of **1** reveals that the unique coupling component makes an angle of either 2° or 58° with respect to the Hg−P bond axis. Choosing the former of these two possibilities as the actual assignment results in an orientation of the phosphorus CS tensor depicted in Figure 3. Examination of the local site symmetry about the phosphorus atom provides further support for this assignment. As is evident in Figure 3, there exists an approximate local mirror plane at the phosphorus atom, bisecting the C(7)−P−C(13) angle. Therefore, one principal component must lie in a direction perpendicular to this plane, while the remaining two components are forced to lie within this plane. Furthermore, the local symmetry of the first coordination sphere about the phosphorus atom contains an approximate C_3 axis, the direction of which corresponds to the Hg−P bond direction. This local symmetry is reflected in the orientation of the CS tensor obtained from our single-crystal ^{31}P NMR study for the assignment depicted in Figure 3 only. Note that the component of intermediate shielding is directed normal to the Hg−P−C(1) plane. The most shielded component, δ_{33}, deviates by only 4° from the direction of the Hg−P bond and the approximate C_3 axis.

(38) Veeman, W. S. *Progr. Nucl. Magn. Reson. Spectrosc.* **1984**, *16*, 193−235.
(39) Kennedy, M. A.; Ellis, P. D. *Concepts Magn. Reson.* **1989**, *1*, 35−47, 109−129.
(40) Mehring, M. *Principles of High Resolution NMR in Solids*, 2nd ed.; Springer-Verlag: Berlin, 1983.
(41) Gerstein, B. C.; Dybowski, C. R. *Transient Techniques in NMR of Solids*; Academic Press: Orlando, FL, 1985.
(42) Power, W. P.; Mooibroek, S.; Wasylishen, R. E.; Cameron, T. S. *J. Phys. Chem.* **1994**, *98*, 1552−1560.

(43) The function of the phase shift, ξ, is to compensate for random error in alignment of the appropriate NMR cube axis in a direction parallel with the external magnetic field direction at the commencement of each rotation. These can be assigned by optimizing the agreement between the spectra obtained at the 90° orientation for rotation about the cube *X* axis, $X(90°)$, and at the 0° position for rotation about the cube *Y* axis, $Y(0)°$, and likewise for the $Y(90°)/Z(0)°$ and $Z(90°)/X(0)°$ orientations.

The principal components of the ^{31}P chemical shift tensor of **1** determined in the present study exhibit an extraordinary sensitivity of the chemical shielding to subtle structural differences. While the principal components perpendicular to the Hg−P bond, δ_{11} and δ_{22}, differ by 30 ppm, all Hg−P−C bond angles and P−C bond distances are rather similar; the difference between the greatest and the smallest Hg−P−C bond angle is only 2°. Since the present study is just the second ^{31}P single-crystal NMR study of a phosphine−metal complex, the lack of well-established benchmarks in addressing chemical shift−structure correlations precludes any attempts to rationalize the results obtained here. The only other single-crystal ^{31}P NMR study of a phosphine−metal complex has been carried out for Wilkinson's catalyst, $Rh(PPh_3)_3Cl$.[44] Unfortunately, Wilkinson's catalyst crystallizes in the space group $Pna2_1$ with four magnetically distinct molecules in the unit cell, which presents a fundamental problem as there are, in principle, twelve possible assignments of the phosphorus shielding tensors to orientations in the molecular frame.[44] At present, we may only state our observation that in **1** δ_{11} is oriented within the plane containing the smallest Hg−P−C bond angle, a pattern which may also hold for $Rh(PPh_3)_3Cl$, pending on the chosen assignment. We do not want to imply that δ_{11} depends on the smallest angle, since the magnitude of shielding in a particular direction depends on the induced currents in the plane normal to this direction. Also, differences of 30 ppm in the individual components of the phosphorus chemical shift tensor are not unusual. For example, for chelate complexes of tungsten, molybdenum, manganese, or platinum it has been shown that principal components may vary over a range of 400 ppm, only dependent on the size of the chelate ring.[45] Finally, it is noteworthy that the chemical shift along the mercury−phosphorus bond, 10−35 ppm, observed for **1** and other mercury complexes,[18,20,21] is rather unusual as compared to phosphine complexes of other transition metals. Typically, the most shielded direction is associated with values of −20 to −80 ppm (M = Mo, W, Mn, Rh, Fe, Ni)[44-46] or 0 to −20 ppm (M = Pt).[22,47]

$^{199}Hg-^{31}P$ J Tensors. The magnitude of the observed $^{199}Hg-^{31}P$ spin−spin coupling, $\Delta\nu$, for a given orientation of the single crystal of **1** in the external magnetic field is a function of both the direct and indirect coupling interactions (*cf.* eq 1). Obviously, the anisotropic component of the $^{199}Hg-^{31}P$ spin−spin coupling is independent of the isotropic J coupling constant. Consequently, in analyzing the ^{199}Hg satellite splittings in the single-crystal NMR spectra, $^1J(^{199}Hg,^{31}P)_{iso}$ was first subtracted from the observed splittings, which isolates the magnitude of the coupling due to the direct dipolar and **anisotropic** indirect spin−spin coupling, exclusively. This quantity is commonly referred to as an *effective* dipolar coupling. Given the characteristic magnitude of isotropic $^{199}Hg-^{31}P$ J couplings in 1:1 mercury−phosphine complexes (*ca.* 8−10 kHz), $^1J(^{199}Hg,^{31}P)_{iso}$ was expected to be an extremely sensitive function of the electronic structure in the vicinity of the Hg−P bond. Therefore, this parameter has been measured from an MAS spectrum of the same single crystal used throughout this study. The value obtained, 8199 ± 25 Hz, is identical, within experimental error, to that obtained from an MAS spectrum for a powdered sample of **1**. It is interesting that the isotropic J coupling measured in the earlier ^{31}P NMR investigation alluded to in the previous section,[21] $^1J(^{199}Hg,^{31}P)_{iso}$ = 8008 Hz, differs significantly from that obtained here which, once again, must be attributed to the use of the two distinct structural isomers in each of these studies.

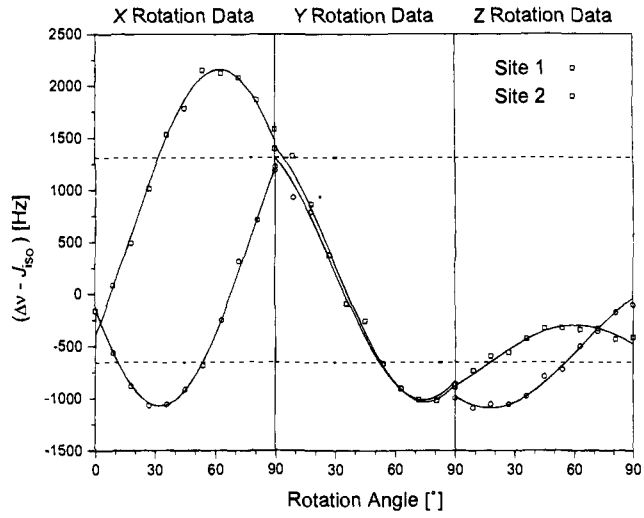

Figure 6. NMR single-crystal rotation plots displaying the variation in the $^{199}Hg-^{31}P$ effective dipolar coupling for rotations about the cube X, Y, and Z axes, as indicated. The calculated range of the direct $^{199}Hg-^{31}P$ dipolar coupling, based on the Hg−P bond length determined from the present X-ray crystallographic study, is indicated by dashed lines. The data obtained for each magnetically nonequivalent site are labeled according to the scheme depicted in Figure 2.

Rotation patterns showing the variation in the $^{199}Hg-^{31}P$ effective dipolar coupling for rotation about the three orthogonal cube axes are illustrated in Figure 6. These data were analyzed in an analogous fashion to the phosphorus CS tensor data outlined in the previous section except that the value for the chemical shift was replaced by the magnitude of the $^{199}Hg-^{31}P$ effective dipolar coupling (in hertz). It should be mentioned that this analysis assumes **J** to be a symmetric tensor; antisymmetry in **J**[48-50] has never been experimentally detected and even if non-zero, its influence on the observed spectra would undoubtedly be undetectable.[49] The effective dipolar coupling tensors obtained for each of the two magnetically distinct crystallographic sites in the single crystal of **1** are summarized in Table 3 with respect to the orthogonalized crystallographic reference frame, (a^*, b, c). As mentioned in the previous section, although there exist two possible assignments for the orientation of the effective dipolar coupling tensor in the molecular reference frame, with R_{zz}^{eff} lying either approximately 2° or 58° off the Hg−P bond axis, only the former of these two possibilities is intuitively reasonable. Keeping in mind that these results represent the combination of both the traceless part of the **J** tensor and the $^{199}Hg-^{31}P$ dipolar tensor and, furthermore, given the experimental uncertainty associated with R_{xx}^{eff} and R_{yy}^{eff} (*cf.* Table 3), one can therefore immediately conclude that the $^{199}Hg-^{31}P$ **J** tensor in **1** is both axially symmetric and collinear with the dipolar interaction. In other words, the magnitude of the ^{199}Hg satellite splittings, $\Delta\nu$, observed in the ^{31}P single-crystal NMR spectra of **1**, can be expressed as

(44) Naito, A.; Sastry, D. L.; McDowell, C. A. *Chem. Phys. Lett.* **1985**, *115*, 19−23.
(45) (a) Lindner, E.; Fawzi, R.; Mayer, H. A.; Eichele, K.; Hiller, W. *Organometallics* **1992**, *11*, 1033−1043. (b) Lindner, E.; Fawzi, R.; Mayer, H. A.; Eichele, K.; Pohmer, K. *Inorg. Chem.* **1991**, *30*, 1102−1107.
(46) (a) Gobetto, R.; Harris, R. K.; Apperley, D. C. *J. Magn. Reson.* **1992**, *96*, 119−130. (b) Wu, G.; Wasylishen, R. E. *Organometallics* **1992**, *11*, 3242−3248. (c) Randall, L. H.; Carty, A. J. *Inorg. Chem.* **1989**, *28*, 1194−1198. (d) Jarrett, P. S.; Sadler, P. J. *Inorg. Chem.* **1991**, *30*, 2098−2104.
(47) Harris, R. K.; McNaught, I. J.; Reams, P.; Packer, K. J. *Magn. Reson. Chem.* **1991**, *29*, 560−572.
(48) (a) Buckingham, A. D.; Love, I. *J. Magn. Reson.* **1970**, *2*, 338−351. (b) Buckingham, A. D.; Pyykkö, P.; Robert, J. B.; Wiesenfeld, L. *Mol. Phys.* **1982**, *46*, 177−182.
(49) Robert, J. B.; Wiesenfeld, L. *Phys. Rep.* **1982**, *86*, 363−401.
(50) Abragam, A.; Goldman, M. *Nuclear Magnetism: Order and Disorder*; Oxford University Press: New York, 1982.

Table 3. Effective $^{199}Hg-^{31}P$ Dipolar Coupling Tensor Data for $HgPCy_3(NO_3)_2$ Obtained from Analysis of the Single-Crystal NMR Data[a]

		effective coupling (Hz)[b]	direction cosines[c]		
site 1	R_{zz}^{eff}	2368	−0.855	0.481	−0.197
	R_{yy}^{eff}	−1010	−0.494	−0.869	0.031
	R_{xx}^{eff}	−1072	−0.156	0.117	0.980
site 2	R_{zz}^{eff}	2288	0.842	0.486	0.230
	R_{yy}^{eff}	−1039	0.051	0.359	−0.934
	R_{xx}^{eff}	−1164	0.537	−0.797	−0.271

[a] The convention used for designating the three principal components of the effective $^{199}Hg-^{31}P$ coupling tensor is $|R_{zz}| \geq |R_{xx}| \geq |R_{yy}|$. [b] Errors in the principal components of the effective $^{199}Hg-^{31}P$ coupling tensors are estimated to be 150 Hz. [c] The direction cosines are with respect to the orthogonalized crystallographic frame (a^*, b, c).

$$\Delta\nu = J_{iso} - R_{eff}(3\cos^2\theta - 1) \quad (2)$$

where R_{eff} is the effective $^{199}Hg-^{31}P$ dipolar coupling constant and θ is the angle between the Hg–P bond axis and the external magnetic field. Furthermore, the magnitude of R_{eff} can be written as

$$R_{eff} = R_{DD} - \Delta J/3 \quad (3)$$

where R_{DD} is the direct $^{199}Hg-^{31}P$ dipolar coupling constant

$$R_{DD} = \frac{\mu_o}{4\pi}\frac{\hbar}{2\pi}\frac{\gamma_{Hg-199}\gamma_{P-31}}{\langle r^3_{Hg-P}\rangle} \quad (4)$$

and ΔJ is the anisotropy in the axially symmetric **J** tensor ($\Delta J = J_{||} - J_{\perp}$). These conclusions will remain implicit throughout the remainder of this discussion.

It is useful to qualitatively examine the rotation plots displayed in Figure 6. Of particular interest are the data obtained for rotation about the cube *X* axis. Examination of the projection of the crystal structure of **1** into the cube *YZ* plane reveals that the Hg–P bond vector is oriented at an angle of approximately 9° with respect to this plane. Since the external magnetic field "moves" within the cube *YZ* plane in this rotation plot, it is clear from eq 2 that the range of $^{199}Hg-^{31}P$ effective coupling will approximate $3R_{eff}$, which is observed experimentally. This result can be compared with that which would be obtained based exclusively on $^{199}Hg-^{31}P$ direct dipolar coupling (*i.e.* $\Delta J = 0$). Such a comparison is depicted in Figure 6, where the calculated limits for the direct dipolar coupling (*cf.* eq 4; $R_{DD} = 665$ Hz) are indicated by dashed lines (for ease of comparison, the sign of R_{DD} was taken to be negative). Unquestionably, the experimental findings presented in Figure 6 clearly demonstrate that the $^{199}Hg-^{31}P$ effective dipolar coupling in **1** possesses a sizable contribution from an anisotropic $^{199}Hg-^{31}P$ **J** tensor. Furthermore, it is important to emphasize that this result provides irrefutable evidence that the **J** tensor is anisotropic; regardless of factors such as motional averaging or the absolute sign of the effective dipolar coupling constant, this conclusion qualitatively remains unaltered.

In order to quantify the contribution from the anisotropic part of the $^{199}Hg-^{31}P$ **J** tensor to the effective dipolar coupling, knowledge of the absolute sign of the latter term is necessary. Although this information is not directly accessible from the results of the present experiment, the relative signs of $^1J(^{199}Hg,^{31}P)_{iso}$ and R_{eff} can be deduced. The fact that maximum and minimum splittings of approximate magnitude $|^1J_{iso}| + 2|R_{eff}|$ and $|^1J_{iso}| - |R_{eff}|$, respectively, are experimentally observed (*cf.* Figure 6) requires that $^1J_{iso}$ and R_{eff} be of opposite sign. Consequently, since $^1J(^{199}Hg,^{31}P)_{iso}$ has previously been found to be positive,[3,51–53] the absolute sign of the effective $^{199}Hg-^{31}P$ dipolar coupling is concluded to be negative. With this information, the contribution from the known $^{199}Hg-^{31}P$ direct dipolar coupling can be separated from the effective coupling tensor to isolate the traceless component of the $^{199}Hg-^{31}P$ **J** tensor. The results of this analysis are summarized in Table 4. It should be emphasized that the components of this tensor are isolated from contributions due to the Fermi contact

Table 4. The Three Principal Components of the Traceless Part of the $^{199}Hg-^{31}P$ **J** Tensor (in Hz) for $HgPCy_3(NO_3)_2$ Obtained from Analysis of the Single-Crystal NMR Data[a]

	site 1	site 2
$J_{zz} - J_{iso}$	3698	3618
$J_{yy} - J_{iso}$	−1675	−1704
$J_{xx} - J_{iso}$	−1737	−1829
ΔJ	5404	5385

[a] Obtained from the effective dipolar coupling tensor (*cf.* Table 3) by subtracting out the direct dipolar coupling contribution. The convention used for designating the three principal components of the $^{199}Hg-^{31}P$ **J** tensor is $|J_{zz} - J_{iso}| \geq |J_{xx} - J_{iso}| \geq |J_{yy} - J_{iso}|$. Errors in the above numbers are estimated to be 150 Hz.

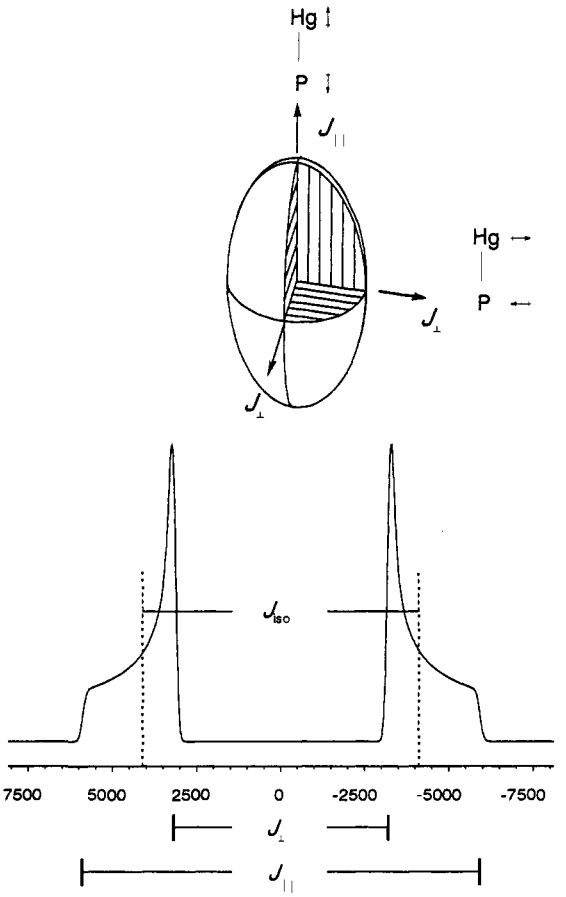

Figure 7. A hypothetical ^{31}P NMR powder spectrum for **1**, obtained by considering the $^{199}Hg-^{31}P$ indirect spin–spin coupling interaction only. The anisotropy in the **J** tensor, which is illustrated in the conventional ellipsoidal representation, was taken to be 5.4 kHz. The magnitudes of the indicated couplings are as follows: $J_{||} = 11.8$ kHz, $J_{\perp} = 6.4$ kHz, and $J_{iso} = 8.2$ kHz.

(51) Verkade, J. G.; Mosbo, J. A. In *Phosphorus-31 NMR Spectroscopy in Stereochemical Analysis, Organic Compounds and Metal Complexes*; Verkade, J. G., Quin, L. D., Eds.; Methods in Stereochemical Analysis 8; VCH Publishers, Inc.: Deerfield Beach, FL, 1987; p 425.
(52) McFarlane, W.; Rycroft, D. S. *J. Chem. Soc., Faraday Trans. 2* **1974**, *70*, 377–385.
(53) Goggin, P. L.; Goodfellow, R. J.; McEwan, D. M.; Griffiths, A. J.; Kessler, K. *J. Chem. Res.*, Miniprint **1979**, 2315–2343.

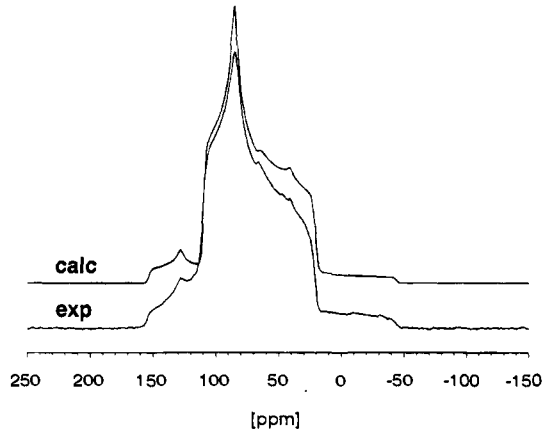

Figure 8. The experimental (bottom) and calculated (top) ^{31}P NMR spectrum for a static powder sample of **1** at an applied field strength of 4.7 T. The calculated spectrum was obtained using the following parameters, obtained from the single-crystal NMR analysis; $\delta_{11} = 110$ ppm, $\delta_{22} = 84$ ppm, $\delta_{33} = 21$ ppm, $J_{iso} = +8199$ Hz, $R_{eff} = -1135$ Hz, $\alpha = 0°$, and $\beta = 4°$.

interaction. Clearly, other mechanism(s) are operative, and furthermore, these make significant contributions to the electron-mediated transfer of nuclear spin information involving ^{199}Hg and ^{31}P nuclei in **1**.

At this point, it is instructive to examine qualitatively the implications of a $^{199}Hg-^{31}P$ J coupling with an anisotropy of 5.4 kHz. For this purpose, consider a hypothetical ^{31}P NMR spectrum for a powder sample of **1** in the absence of both phosphorus chemical shielding and $^{199}Hg-^{31}P$ direct dipolar coupling. In Figure 7, the $^{199}Hg-^{31}P$ **J** tensor has been illustrated in the conventional ellipsoidal representation. When the magnetic field lies parallel to the Hg−P bond, the J coupled nuclei are polarized parallel to the Hg−P bond axis, yielding a J coupling of $J_{\parallel} = 11.8$ kHz (see Figure 7). However, when the magnetic field lies normal to this axis, the spins are aligned in a direction perpendicular to the Hg−P bond axis. Under these conditions, the observed J coupling is $J_{\perp} = 6.4$ kHz. Finally, it is clear that when the spins are polarized at the magic angle ($\theta = 54.7°$) with respect to the Hg−P bond axis, the isotropic J coupling, $J_{iso} = 8.2$ kHz, is observed. Considering all possible orientations of the Hg−P bond axis over the surface of the ellipse in this fashion gives rise to the powder spectrum depicted in Figure 7.

In an effort to perform an independent verification of the single-crystal NMR results obtained here, ^{31}P NMR spectra for a static powder sample of **1** have been obtained at applied field strengths of 4.7 and 9.4 T. The spectrum obtained at 4.7 T is presented in Figure 8. Also illustrated in this same figure is the calculated line shape obtained using the parameters extracted from analysis of the single-crystal NMR data. Details concerning the method of NMR line shape calculations employed in this laboratory have been described in detail elsewhere.[54] The agreement between the experimental and calculated line shapes at both applied fields is very satisfactory, in support of the single-crystal NMR results. It is apparent from the experimental spectrum in Figure 8 that analysis of such a powder pattern is indeed a non-trivial task. This analysis is further compounded in **1** due to the fact that the ^{199}Hg satellite powder patterns are partially embedded within the central line shape which, as mentioned earlier, arises from anisotropic ^{31}P chemical shielding. Although such a system lends itself amenably to analysis using slow-spinning MAS experiments, clearly the single-crystal NMR experiment is a more general and reliable approach.

The results obtained here for the anisotropy in the $^{199}Hg-^{31}P$ J coupling confirm those of an earlier ^{31}P NMR investigation of a 1:1 mercury−tricyclohexylphosphine complex.[21] There, ΔJ was measured to be 5525 ± 200 Hz from analysis of the ^{31}P NMR line shape obtained for a static powder sample. Similar magnitudes of anisotropic J couplings have also been reported in related complexes containing various phosphine ligands.[18,21] Although the status of the current understanding of indirect spin−spin couplings prohibits both resolution of these anisotropic couplings in terms of the contributing mechanisms and interpretation of the origin of the observed experimental trends, it is quite clear that several examples are available where non-contact contributions have been elucidated and that caution must be exercised when interpreting such couplings using concepts stemming from the assumption of Fermi contact dominance. This certainly appears to hold true for J couplings involving the heavier metal nuclei. Although reliable theoretical calculations of **J** tensors in such systems would be invaluable to our understanding of these experimental findings, it is unfortunate that systems such as these impose formidable barriers to a successful theoretical treatment. Nevertheless, it is anticipated that reliable experimental measurements of **J** tensors, as in the present investigation, will compel theoreticians to intensify their efforts in advancing the current level of theory concerning the calculation of indirect spin−spin coupling tensors. To this end, further single-crystal NMR measurements of **J** tensors are presently underway in our laboratory.

Acknowledgment. We thank the Natural Sciences and Engineering Research Council of Canada (NSERC) for financially supporting this research in the form of operating and equipment grants (R.E.W. and T.S.C.) as well as a postgraduate scholarship (M.D.L.). K.E. and M.D.L. thank both Dalhousie University and the Izaak Walton Killam Trust for a postdoctoral fellowship and a postgraduate scholarship, respectively. Mr. Pradip Bakshi is gratefully acknowledged for his assistance with some of the X-ray crystallographic aspects of this study. All experimental NMR spectra were acquired at the Atlantic Region Magnetic Resonance Centre.

Supplementary Material Available: A listing of positional parameters, thermal parameters, bond lengths, bond angles, and torsional angles (8 pages). This material is contained in many libraries on microfiche, immediately follows this article in the microfilm version of the journal, and can be ordered from the ACS; see any current masthead page for ordering information.

(54) See, for example: Eichele, K.; Wasylishen, R. E. *J. Magn. Reson. A* **1994**, *106*, 46−56.